QCD THERMODYNAMICS: CONFRONTING THE POLYAKOV-QUARK–MESON MODEL WITH LATTICE QCD*

J. Wambach[a], B.-J. Schaefer[b], M. Wagner[a,c]

[a]Institut für Kernphysik, TU Darmstadt, 64289 Darmstadt, Germany
[b]Institut für Physik, Karl-Franzens-Universität, 8010 Graz, Austria
[c]ExtreMe Matter Institute EMMI, GSI Helmholtzzentrum für Schwerionenforschung GmbH, 64291 Darmstadt, Germany

NJL-type effective models represent a low-energy realization of QCD and incorporate pertinent aspects such as chiral symmetry and its spontaneous breaking, the center symmetry in the heavy-quark limit as well as the axial anomaly. One such model, the Polyakov-quark–meson model for three light quark flavors, is introduced in order to study the phase structure of strongly-interacting matter. With recent high-statistics lattice QCD simulations of the finite-temperature equation of state, a detailed comparison with model results becomes accessible. Such comparisons allow to estimate volume and truncation effects of quantities, obtained on the lattice and provide possible lattice extrapolation procedures to finite chemical potential which are important to locate a critical endpoint in the QCD phase diagram.

PACS numbers: 12.38.Aw, 11.10.Wx, 11.30.Rd, 12.38.Gc

1. Introduction

A detailed theoretical understanding of strongly-interacting matter under extreme conditions is mandatory for various heavy-ion research programs. The search for possible (tri)critical endpoints in the phase diagram is a major focus of the CBM experiment at the future FAIR facility.

Different regimes of the QCD phase diagram can be explored by employing various theoretical methods. Lattice QCD simulations are applicable at zero or imaginary chemical potentials. Most simulations for $(2+1)$ flavor QCD agree that chiral symmetry is restored by a smooth crossover

---

transition at $\mu = 0$ [1] but there is still an ongoing discussion concerning the (pseudo)critical temperatures [2]. At finite real chemical potentials the fermion sign problem remains a considerable obstacle. Several extrapolation techniques to finite chemical potentials such as the reweighting method, imaginary chemical potential or a Taylor expansion around vanishing chemical potentials have been proposed (for an overview see [3]). Effective models, such as the Polyakov loop NJL (PNJL) or the Polyakov-loop quark–meson (PQM) model [4], incorporate important fundamental symmetries and the symmetry breaking pattern of the underlying QCD but do not suffer from the sign problem, large quark masses or finite volume restrictions. Furthermore, these type of models can be used to test certain lattice extrapolation techniques to finite μ. For this purpose the reproduction of the lattice data for vanishing μ is a basic prerequisite.

In this paper we compare the bulk thermodynamics of several chiral $N_f = 2 + 1$ quark flavor PQM models with recent $N_\tau = 8$ lattice data of the HotQCD Collaboration [5]. The larger quark masses used on the lattice are explicitly considered in the model comparison. Based on a novel differentiation technique, higher derivatives of the thermodynamic potential can be calculated very precisely [6]. This method allows to investigate convergence properties of the Taylor expansion method used on the lattice.

2. Polyakov–quark–meson model

The Polyakov-quark–meson (PQM) model for three quark flavors is based on the linear σ-model with quarks [7] and incorporates in addition the Polyakov-loop field $\Phi(\vec{x})$. The Polyakov loop is the thermal expectation value of a color traced Wilson loop in the temporal direction. In the heavy-quark limit Φ serves as an order parameter for the confinement/deconfinement transition. In the deconfined high-temperature phase the center symmetry $Z(3)$ of QCD is spontaneously broken and as a consequence Φ is finite. However, with dynamical quarks the center symmetry is always broken and Φ as an order parameter becomes questionable.

The PQM Lagrangian consists of a quark–meson (QM) contribution and a Polyakov-loop potential $\mathcal{U}(\Phi, \bar{\Phi})$, which depends on Φ and its Hermitian conjugate $\bar{\Phi}$. The uniform temporal background gauge field is coupled to the quarks by replacing the standard derivative ∂_μ in the quark contribution by a covariant derivative $D_\mu = \partial_\mu - iA_\mu$, $A_\mu = \delta_{\mu 0}A^0$ where $A_\mu \equiv g_s A_\mu^a \lambda^a / 2$. This leads to the Lagrangian

$$\mathcal{L}_{\text{PQM}} = \bar{q}\left(i\slashed{D} - g\phi_5\right)q + \mathcal{L}_m - \mathcal{U}(\Phi[A], \bar{\Phi}[A]), \tag{1}$$

where q denotes the quark field. The interaction between the quarks and the meson nonets is implemented by a flavor-blind Yukawa coupling g and the meson matrix $\phi_5 = \sum_{a=0}^{8}(\lambda_a/2)\,(\sigma_a + i\gamma_5\pi_a)$ where the nine scalar mesons fields are labeled by σ_a and accordingly the nine pseudoscalar fields by π_a.

The remaining, purely mesonic contribution reads

$$
\begin{aligned}
\mathcal{L}_m \;=\; & \mathrm{Tr}\left(\partial_\mu\phi^\dagger\partial^\mu\phi\right) - m^2\,\mathrm{Tr}(\phi^\dagger\phi) - \lambda_1\left[\mathrm{Tr}(\phi^\dagger\phi)\right]^2 - \lambda_2\,\mathrm{Tr}\left(\phi^\dagger\phi\right)^2 \\
& + c\left(\det(\phi) + \det(\phi^\dagger)\right) + \mathrm{Tr}\left[H(\phi + \phi^\dagger)\right],
\end{aligned}
\tag{2}
$$

with the fields $\phi \equiv \sum_a(\lambda_a/2)\,(\sigma_a + i\pi_a)$. Chiral symmetry is explicitly broken by the last term in Eq. (2) and the $U(1)_A$-symmetry by the 't Hooft determinant term with constant strength c.

For the effective Polyakov-loop potential $\mathcal{U}$ which is constructed in terms of Φ and $\bar{\Phi}$, several implementations are available. The simplest choice is based on a Ginzburg–Landau ansatz [8]:

$$
\frac{\mathcal{U}_{\mathrm{poly}}}{T^4} = -\frac{b_2}{4}\left(|\Phi|^2 + |\bar{\Phi}|^2\right) - \frac{b_3}{6}(\Phi^3 + \bar{\Phi}^3) + \frac{b_4}{16}\left(|\Phi|^2 + |\bar{\Phi}|^2\right)^2.
\tag{3}
$$

The cubic Φ terms are required to break the $U(1)$ symmetry of the remaining terms down to the center symmetry, $Z(3)$. The potential parameters are adjusted to the pure gauge lattice data such that the equation of state and the Polyakov-loop expectation values at finite temperature are reproduced. An improved version [9] based on the SU(3) Haar measure results in

$$
\frac{\mathcal{U}_{\mathrm{log}}}{T^4} = -\frac{1}{2}a(T)\bar{\Phi}\Phi + b(T)\ln\left[1 - 6\bar{\Phi}\Phi + 4\left(\Phi^3 + \bar{\Phi}^3\right) - 3\left(\bar{\Phi}\Phi\right)^2\right].
\tag{4}
$$

The parameters are again fitted to the pure gauge lattice data. The logarithmic form constrains Φ and $\bar{\Phi}$ to values smaller than one. Another choice invented by Fukushima [10] is

$$
\frac{\mathcal{U}_{\mathrm{Fuku}}}{T^4} = -\frac{b}{T^3}\left[54e^{-a/T}\Phi\bar{\Phi} + \ln\left(1 - 6\Phi\bar{\Phi} - 3(\Phi\bar{\Phi})^2 + 4\left(\Phi^3 + \bar{\Phi}^3\right)\right)\right]
\tag{5}
$$

with only two parameters a and b. The parameters also result in a first-order transition at $T_0 \sim 270\,\mathrm{MeV}$ in the pure gauge sector but are not fitted to lattice data. This potential excludes contributions of the unconfined transverse gluons to the equation of state which are relevant at high temperatures [10]. This is important for the comparison to lattice data at higher temperatures.

2.1. Thermodynamic potential

For three quark flavors the grand potential Ω is a function of the temperature and in general three quark chemical potentials, one for each flavor. Here we focus on a uniform quark chemical potential $\mu \equiv \mu_q = \mu_B/3$. Since we consider the isospin-symmetric case with $m_l \equiv m_u = m_d$, only two order parameters, the non-strange σ_x and strange σ_y emerge [7]. The thermodynamic potential in mean-field consists of three different contributions [11]: the mesonic part $U(\sigma_x, \sigma_y)$, a quark part $\Omega_{\bar{q}q}$ and the Polyakov-loop potential

$$\Omega = U\left(\sigma_x, \sigma_y\right) + \Omega_{\bar{q}q}\left(\sigma_x, \sigma_y, \Phi, \bar{\Phi}\right) + \mathcal{U}\left(\Phi, \bar{\Phi}\right) . \tag{6}$$

The mesonic contribution has six parameters which are fitted to the vacuum. For example, the Yukawa coupling g is fixed to reproduce a light constituent quark mass of $m_l \approx 300$ MeV. This then yields a strange constituent quark mass of $m_s \approx 433\,\text{MeV}$.

The temperature- and quark chemical potential dependence of the four order parameters for the chiral and confinement/deconfinement transition are determined as solutions of the corresponding gap equations. These coupled equations are obtained by minimizing the grand potential, Eq. (6), with respect to the four constant mean-fields $\langle \sigma \rangle_x$, $\langle \sigma \rangle_y$, $\langle \Phi \rangle$ and $\langle \bar{\Phi} \rangle$:

$$\frac{\partial \Omega}{\partial \sigma_x} = \frac{\partial \Omega}{\partial \sigma_y} = \frac{\partial \Omega}{\partial \Phi} = \left.\frac{\partial \Omega}{\partial \bar{\Phi}}\right|_{\text{min}} = 0 , \tag{7}$$

where $\text{min} = \left\{\sigma_x = \langle\sigma_x\rangle, \sigma_y = \langle\sigma_y\rangle, \Phi = \langle\Phi\rangle, \bar{\Phi} = \langle\bar{\Phi}\rangle\right\}$ labels the global minimum.

3. Lattice comparison

In order to compare our model results with recent HotQCD lattice findings [5] we have chosen a model parameter setup where the chiral and deconfinement transition temperature coincide at $\mu = 0$. This is the case for $m_\sigma = 600\,\text{MeV}$ and $T_0 = 270\,\text{MeV}$ for all used Polyakov-loop potentials [11]. A coincidence of both transitions around $T_\chi \sim 185$–195 MeV is also observed in the corresponding lattice simulations [5]. However, on the lattice a ratio of the physical strange quark mass to the light one of 10 has been used which yields finally too heavy light-quark masses. For a proper comparison we have therefore adjusted the pion and kaon masses in the model calculations accordingly and use also $m_K = 503\,\text{MeV}$ and $m_\pi = 220\,\text{MeV}$. Of course, heavier meson masses yield also slightly heavier constituent quark masses

$$m_l \approx 322\text{MeV} \qquad \text{and} \qquad m_s \approx 438\text{MeV} .$$

As a consequence, higher transition temperatures, in particular for the chiral transition in the light sector, are found. But both transitions, the non-strange chiral and the deconfinement one, still coincide. The strange quark sector is almost unaffected [11].
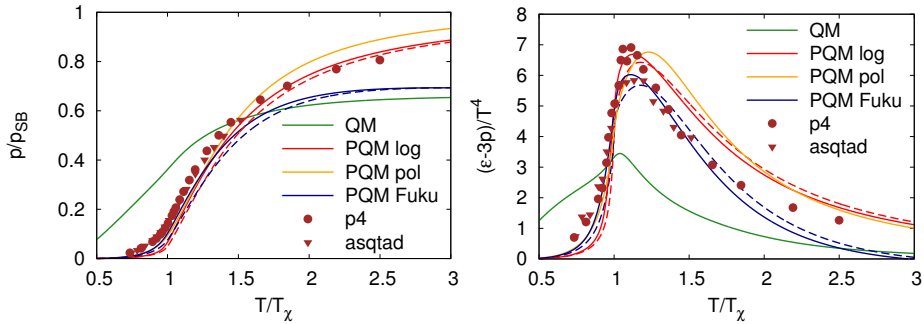

Fig. 1. The normalized pressure p/p_{SB} (left panel) and the interaction measure Δ/T^4 (right panel) as a function of temperature. The model calculations (PQM model with various Polyakov-loop potentials and the QM model) are compared to lattice data ($N_\tau = 8$, p4 and asqtad actions) from [5]. The solid lines correspond to larger pion and kaon masses as used in the lattice simulations while the dashed lines denote the results for physical masses.

In the model calculations all thermodynamic quantities are extracted from the grand potential. The pressure

$$p(T,\mu) = -\Omega\left(T,\mu\right) \tag{8}$$

is directly related to the thermodynamic potential with a suitable normalization, $p(0,0) = 0$. In Fig. 1 the pressure, normalized to the Stefan–Boltzmann (SB) value of the PQM model, is compared to the lattice data and a quark–meson model calculation. As expected, the QM model [7] fails in describing the lattice data, while the PQM model results are in better agreement with the data. The best agreement is achieved with Fukushima's potential where the different treatment of the transverse gluons at higher temperatures is apparent. Around the transition the model versions with the polynomial or logarithmic Polyakov-loop potential are closer to the lattice data. For physical meson masses (dashed lines) the pressure is smaller.

The interaction measure, $\Delta = e - 3p$, indicates the breaking of scale invariance and is given as a temperature derivative of the grand potential

$$\frac{\Delta}{T^4} = T\frac{\partial}{\partial T}\left(\frac{p}{T^4}\right) = -T\frac{\partial}{\partial T}\left(\frac{\Omega}{T^4}\right). \tag{9}$$

In lattice simulations, this quantity can be obtained directly from the trace of the energy-momentum tensor

$$\frac{\Theta^\mu_\mu}{T^4} = \frac{\varepsilon - 3p}{T^4} = \frac{\Delta}{T^4}. \tag{10}$$

It is more sensitive to finite volume and discretization effects than, *e.g.*, the pressure (*cf.* [5]) which is displayed in Fig. 1(b). In the chirally broken phase, the lattice data are close to all model curves. Around the transition $T \approx T_\chi$ Fukushima's potential is closest to the asqtad-action data, while the remaining two model curves are in better agreement with the p4-action data. In general, the peak height decreases on larger lattices, in particular for the p4-action while the asqtad-action shows a weaker N_τ dependence [5]. In contrast to the pressure, the logarithmic and polynomial Polyakov model version do not describe the lattice data in the symmetric phase. However, Fukushima's ansatz approaches the data at least up to $T \sim 1.5 T_\chi$.

In addition we also show the energy density ε and the entropy density s, which are defined as

$$\varepsilon = -p + Ts, \qquad s = -\frac{\partial \Omega}{\partial T}, \tag{11}$$

in Fig. 2 as a function of temperature. Similar to the pressure, Fukushima's potential model version comes closest to the lattice data for $T \lesssim 1.5 T_\chi$.
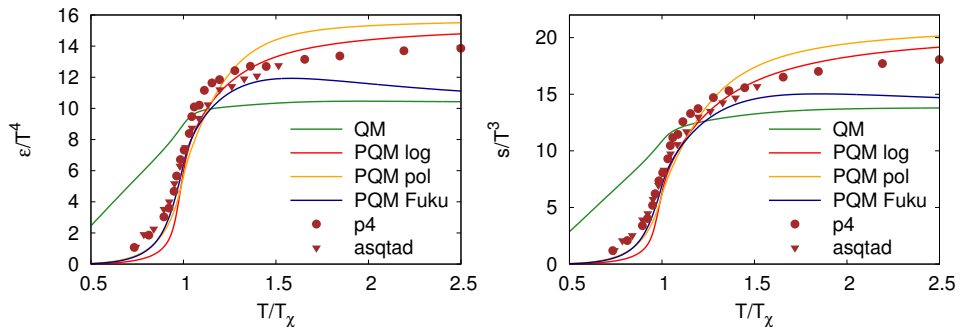

Fig. 2. The energy density ε/T^4 (left panel) and entropy density s/T^3 (right panel) similar to Fig. 1.

4. Convergence of the Taylor expansion at finite μ

At finite chemical potential the spectrum of the Dirac operator becomes complex making direct Monte Carlo simulations impossible. Several methods have been developed to circumvent this problem and to access at least a region of small chemical potentials in the phase diagram, see *e.g.* [3].

One such approach is based on the Taylor expansion of thermodynamic quantities in powers of (μ/T) around $\mu = 0$. For the pressure it reads

$$\frac{p(\mu/T)}{T^4} = \sum_{n=0}^{\infty} c_n(T) \left(\frac{\mu}{T}\right)^n \tag{12}$$

with the coefficients

$$c_n(T) = \frac{1}{n!} \left. \frac{\partial^n \left(p(T,\mu)/T^4\right)}{\partial \left(\mu/T\right)^n} \right|_{\mu=0} . \tag{13}$$

Note that only even coefficients contribute since the QCD partition function is CP-symmetric, *i.e.*, $Z(\mu) = Z(-\mu)$. The coefficients have been calculated up to the eighth order by different lattice groups, for $N_f = 2$ see *e.g.* [12] and for $N_f = 2 + 1$ quark flavors, see *e.g.* [13]. However, higher orders still suffer from large errors.

The application of the Taylor expansion method to the PQM model provides an opportunity to investigate and test the finite μ extrapolation since a direct evaluation of the thermodynamic potential in the model is possible. For example, the location of the critical endpoint (CEP) is exactly known in the model calculation. This enables us to distinguish between divergences related to the CEP and to the breakdown of the expansion.

However, a further difficulty emerges in the model analysis: in principle, the grand potential is known analytically but an analytic evaluation of the Taylor coefficients fails since the implicit temperature and chemical potential dependence of the order parameters is only known numerically via the equations of motion Eq. (7).

Standard methods for an evaluation of numerical derivatives are hampered by increasing errors, which become dominant in particular for higher derivative orders. In order to circumvent this caveat we have developed a novel numerical technique which is based on algorithmic differentiation (AD). With this method the evaluation of higher derivatives becomes feasible to extremely high precision. In fact, it is essentially limited only by machine precision. Details of this method can be found in Ref. [6].

With this method we could obtain the Taylor coefficients up to 22-nd order for the PQM model with the logarithmic Polyakov-loop potential as shown in Fig. 3. The coefficients are very small far away from the transition temperature and they start to oscillate with increasing amplitude within a narrow temperature range around the transition temperature, *i.e.* $0.95\,T_\chi < T < 1.05\,T_\chi$. This signals a complex μ singularity of the thermodynamic potential close to the real axis. In the chiral limit this singularity would be exactly on the real axis as a reflection of a real phase transition.
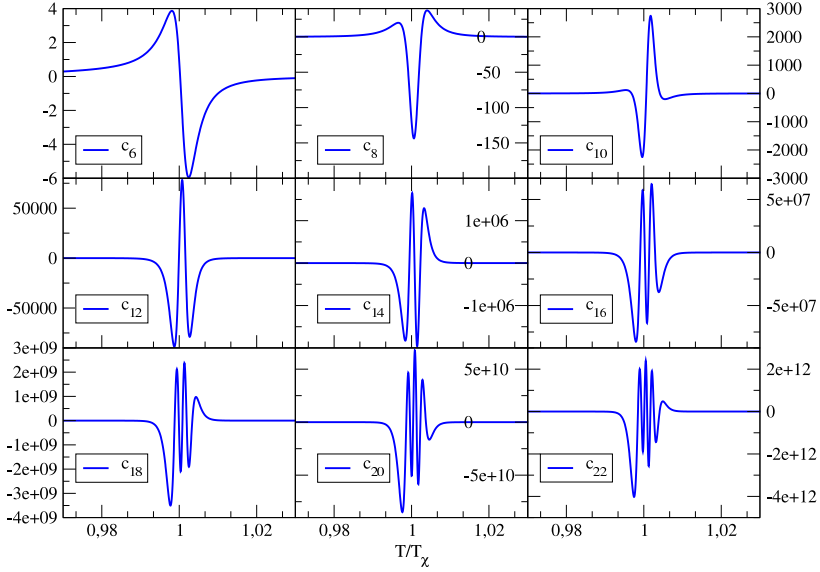
Fig. 3. The Taylor coefficients c_6 to c_{22} obtained in the PQM model with the logarithmic Polyakov-loop potential ($T_0 = 270\,\mathrm{MeV}, m_\sigma = 600\,\mathrm{MeV}$).

By means of the Taylor expansion method it is further possible to study several thermodynamic quantities at small μ. One example is the pressure difference

$$\frac{\Delta p(T, \mu)}{T^4} = \frac{p(T, \mu) - p(0, 0)}{T^4} = \sum_{n=2,4,\dots} c_n(T) \left(\frac{\mu}{T}\right)^n . \tag{14}$$

In Fig. 4 we show Δp for $\mu/T = 0.8$ and $\mu/T = 1.0$ for various expansion orders in comparison with the model result. The ratios μ/T are slightly below and above the critical value $\mu_c/T_c \sim 0.9$ at the CEP. Although the transition is still a crossover at $\mu/T = 0.8$, a divergence is observed in the Taylor expansion. The divergence becomes more prominent with increasing orders. However, a direct model evaluation of the pressure, labeled as "PQM" in the figure, shows a smooth behavior. The divergence in the coefficients is clearly a signal for the breakdown of the Taylor expansion, which is also related to the oscillations in the coefficients. This occurs already for $\mu/T < 1$ and indicates the importance of the higher order coefficients. For temperatures just below the breakdown at $T \sim 0.95\,T_\chi$ the higher orders improve the observed agreement with the "PQM" curve. A similar behavior is also seen for the $\mu/T = 1$ case. At higher temperatures $T \gg T_\chi$ the coefficients become small again and do not longer contribute. As a consequence the Taylor expansion can again reproduce the PQM result.
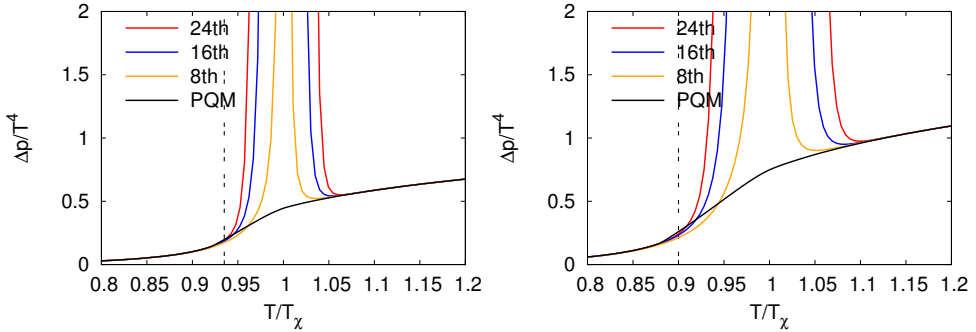
Fig. 4. The pressure difference $\Delta p/T^4$ for different ratios of μ/T (left panel $\mu/T = 0.8$, right panel $\mu/T = 1.0$) and orders of the Taylor expansion. The black line, labeled with "PQM", is the model calculation. The vertical dashed line indicates the radius of convergence.

For a deeper understanding of the breakdown of the Taylor expansion it is instructive to investigate its convergence radius. It can be obtained from the definition

$$r = \lim_{n \to \infty} r_{2n} = \lim_{n \to \infty} \left| \frac{c_{2n}}{c_{2n+2}} \right|^{1/2} . \tag{15}$$

It is not yet known how well the radius r is estimated by r_n for a finite value n. The estimated r_{24} is indicated by the dashed vertical line in Fig. 4. It coincides with the occurrence of the divergence observed in Δp at 24th order. From the different r_n we expect that the true convergence radius is smaller than r_{24} for the given μ/T ratios. For more details see [14]. A detailed study concerning the prospects of locating the CEP within the Taylor expansion will be given in [15].

5. Summary

In this paper we have presented results for the bulk thermodynamics of a $(2 + 1)$ flavor PQM model with three different effective Polyakov-loop potentials. The model parameters are adjusted at vanishing chemical potential to produce a coincidence of the chiral and deconfinement transition for all three Polyakov-loop potentials. For a better comparison with the recent HotQCD lattice data we further tuned the pion and Kaon masses to these values which are used in the lattice simulations. All three PQM model versions yield a good reproduction of the lattice data for temperatures $T < 1.5 \, T_\chi$. Furthermore, the Taylor expansion of the pressure difference for finite chemical potentials is also investigated. For this purpose, a novel algorithmic differentiation technique has been developed. The Taylor

coefficients up to 24th order could be obtained in the PQM model for the first time. The knowledge of these higher Taylor coefficients allows for a systematic study of convergence properties of the expansion.

REFERENCES

[1] Y. Aoki *et al., Nature* **443**, 675 (2006).

[2] M. Cheng *et al., Phys. Rev.* **D74**, 054507 (2006); Y. Aoki *et al., J. High Energy Phys.* **06**, 088 (2009).

[3] O. Philipsen, *PoS* **LAT2005**, 016 (2006); C. Schmidt, *PoS* **LAT2006**, 021 (2006).

[4] B.-J. Schaefer, J.M. Pawlowski, J. Wambach, *Phys. Rev.* **D76**, 074023 (2007).

[5] A. Bazavov *et al., Phys. Rev.* **D80**, 014504 (2009).

[6] M. Wagner, A. Walther, B.-J. Schaefer, *Comput. Phys. Commun.* **181**, 756 (2010).

[7] B.-J. Schaefer, M. Wagner, *Phys. Rev.* **D79**, 014018 (2009).

[8] C. Ratti, M.A. Thaler, W. Weise, *Phys. Rev.* **D73**, 014019 (2006).

[9] S. Roessner, C. Ratti, W. Weise, *Phys. Rev.* **D75**, 034007 (2007).

[10] K. Fukushima, *Phys. Rev.* **D77**, 114028 (2008).

[11] B.-J. Schaefer, M. Wagner, J. Wambach, `arXiv:0910.5628[hep-ph]`.

[12] C.R. Allton *et al., Phys. Rev.* **D71**, 054508 (2005); R.V. Gavai, S. Gupta, *Phys. Rev.* **D78**, 114503 (2008); R.V. Gavai, S. Gupta, *Phys. Rev.* **D71**, 114014 (2005).

[13] C. Miao, C. Schmidt, [RBC-Bielefeld Collaboration], *PoS* **LAT2008**, 172 (2008).

[14] B.-J. Schaefer, M. Wagner, J. Wambach, *PoS* **CPOD2009**, 017 (2009).

[15] F. Karsch, B.-J. Schaefer, M. Wagner, J. Wambach, in preparation.